



Risks of Solely Relying on V_{s30} in Ground Motion Response Studies

Amin Ghanbari ^{a*}, Younes Daghigh ^b, Forough Hassanvand ^a

^a Graduate Student, Department of Civil Engineering, Islamic Azad University, Tehran, Iran.

^b Assistant Professor, Department of Civil Engineering, Islamic Azad University, Karaj, Iran.

Received 02 July 2018; Accepted 17 November 2018

Abstract

The average shear wave velocity of the uppermost 30 m of earth (V_{s30}) is widely used in seismic geotechnical engineering and soil-structure interaction studies. In this regard, any given subsurface profile is assigned to a specific site class according to its average shear wave velocity. However, in a real-world scenario, entirely different velocity models could be considered in the same class type due to their identical average velocities. The objective of the present study is to underline some of the risks associated with solely using V_{s30} as a classification tool. To do so, three imaginary soil profiles that are quite different in nature, but all with the same average V_s were considered and were subjected to the same earthquake excitation. Seismic records acquired at the ground surface demonstrated that the three sites have different ground motion amplifications. Then, the different ground responses were used to excite a five-story structure. Results confirmed that even sites from the same class can indeed exhibit different responses under identical seismic excitations. Our results demonstrated that caution should be practiced when large-contrast velocity models are involved as such profiles are prone to pronounced ground motion amplification. This study, which serves as link between soil dynamics and structural dynamics, warns practitioners about the risks associated with oversimplifying the subsurface profile. Such oversimplifications can potentially undermine the safety of existing or future structures.

Keywords: V_{s30} ; Shear-Wave Velocity; Seismic Site Class; Soil-Structure Interaction.

1. Introduction

Stiffness properties of near-surface earthen materials have proven to have a great influence on seismic wave propagation. Specifically, the nature of ground motions at a given site is heavily influenced by the shallowest parts of the subsurface [1-2]. This is the underlying reason that explains why most of the geotechnical and environmental engineering applications focus on the shallowest 30 meters of subsurface [3] and therefore, a proper characterization of the near-surface is critically important. In this regard, shear-wave velocity (V_s) is among the parameters that is widely used as a proxy to soil stiffness. The vertical V_s profile for a given site can be estimated using a variety of different methods including conventional geotechnical subsurface investigations. Examples of geotechnical testing methods that have been used for such application are standard penetration testing (SPT) or cone penetration testing (CPT). Typically, results from the geotechnical tests are correlated to shear-wave velocity by using empirical relations available in the literature [4-6]. However, it has been shown that such indirect calculations are vulnerable to a large degree of uncertainty [7]. Therefore, one method to overcome the uncertainties associated with geotechnical testing techniques is to perform geophysical testing methods such as borehole seismic testing [8, 9], surface wave testing [10-12], and seismic refraction and reflection [13, 14].

* Corresponding author: agce86@gmail.com

 <http://dx.doi.org/10.28991/cej-03091210>

➤ This is an open access article under the CC-BY license (<https://creativecommons.org/licenses/by/4.0/>).

© Authors retain all copyrights.

Many building codes around the globe now rely on the average shear wave velocity of the upper 30 m (V_{s30}) for seismic site classification and also for estimating the site-dependent response spectra. V_{s30} has also been widely adopted in seismic microzonation studies [15-17]. This parameter was first introduced in the US 1994 National Earthquake Hazard Reduction Program (NEHRP) Building Code and can be determined using equation (1). In this equation d_i and V_{si} represent the thickness and V_s of the i^{th} layer (layers stretching from the ground surface to a depth of 30 meters). The NEHRP has provided a definition for site classes as listed in Table 1 [18].

$$V_{s30} = \frac{30 \text{ m}}{\sum_{i=1}^n \frac{d_i}{V_{si}}} \quad (1)$$

Table 1. NEHRP site classification using V_{s30} [18]

Soil	Profile Type	V_s (m/s)
A	Hard rock	> 1500
B	Rock	760-1500
C	Very dense soil/soft rock	360-760
D	Stiff soil	180-360
E	Soft soil	< 180
F	Special soil requiring site-specific evaluation	

Arguably, several different subsurface profiles can be found in the nature that possess the same V_{s30} and thus, all will be considered in the same class. However, such profiles can vary significantly from one to another that can change their ground motion responses. Despite the wide use of V_{s30} and some of its strong advocates, there has been some questions and concerns regarding the reliability of V_{s30} . The studies by Wald et al. (2011) and Godfrey et al. (2015) highlighted that V_{s30} might not properly capture the behavior of sharp V_s contrast sites which can lead to underestimation of NEHRP amplification factors obtained from V_s [19-20]. Some of the recent studies have shown that there is considerable uncertainty introduced into ground motion prediction equations due to the use of simple site classes as the decision criteria for amplification factor choice [21]. Moreover, V_{s30} lacks any information pertaining to frequency dependence [19]. Others also have raised doubts as to whether V_{s30} is a reliable tool in seismic amplification studies since seismic amplification is evidently too complex to be lumped up in a single synthetic parameter measured over the top 30 meters of the ground [22-25].

To the best of authors' knowledge, the majority of the published literature is based on results from field surveys and experimental setups and little work has been undertaken in a pure numerical context to explore the hazards of over-relying on V_{s30} . Using a computational framework, the purpose of the present study is therefore to demonstrate the potential risks associated with using V_{s30} as a single seismic classification tool.

2. Methods

As mentioned earlier, the present study is a combination of soil dynamics and structural dynamics. We developed three imaginary soil profiles, all with similar V_{s30} , and subjected them to identical earthquake excitations. The one-dimensional, equivalent linear ground response analysis program ProShake 2.0 was utilized to study the ground response at each site. The program offers a variety of options for soil model. For the purpose of this study, the well-known model by Seed and Idriss (1970) which contains modulus reduction and damping curves for sands was used [26].

Next, the ground responses recorded at the ground surface were used to excite a multi-degree-of-freedom structure, and the differences in the structural response were observed and recorded. A MATLAB code written by [27] was employed to carry out a linear time history analysis of the five-degrees-of-freedom (MDOF) structure. The code solves modal differential equations of motion of a given MDOF structure by using numerical computational techniques such as Newmark's β method and Wilson- θ method. Figure 1 is a flowchart that summarizes the above-mentioned steps.

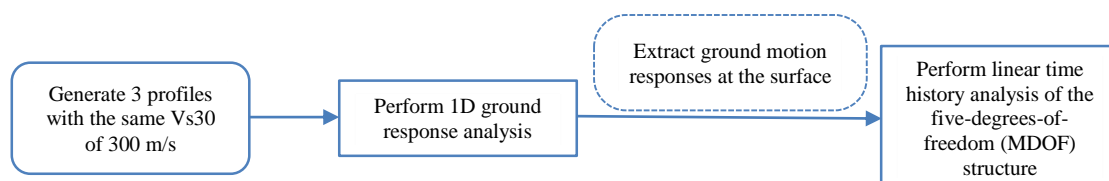


Figure 1. Analysis steps taken in the present study

3. Soil Profiles and Input Ground Motion

The three fictitious V_s profiles that have been examined in this study are shown in Figure 2. All these velocity models have an average shear wave velocity of 300 m/s and therefore, they are all classified as type D soil (stiff soil) according to NEHRP code. Profile 1 consists of a uniform layer of $V_s=300$ m/s. This profile is basically used as a benchmark model. Profile 2 is a two-layer model in which a strong impedance contrast exists between the two layers. Profile 3 is made of 10 layers, each 3 m-thick, and represents a gradual increase in stiffness. V_p profiles were determined assuming a constant Poisson's ratio of 0.33. As for the density of layers, the empirical relation by Ludwig et al. (1970) was used to estimate density values [28]. The density values were then constrained by a lower bound of 1400 kg/m³ meaning that densities below this threshold were increased to 1400 kg/m³. A detailed list of properties from these velocity models is summarized in Table 2.

Using ProShake, all the sites were subjected to the excitation from 1940 El Centro earthquake (Figure 3). The input excitation was introduced at a depth of 30 m in all the three profiles, and thus, only the upper 30 m of subsurface is involved in the ground motion response analysis.

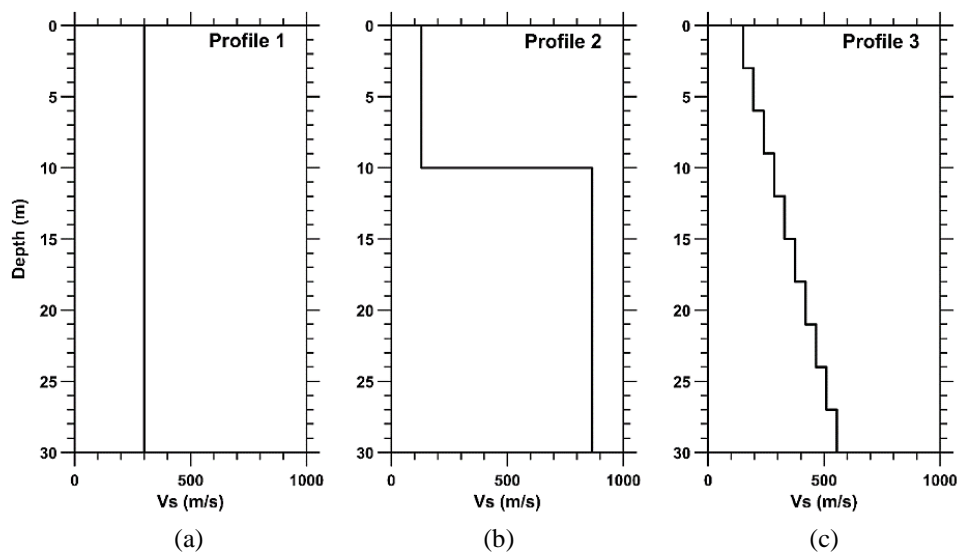


Figure 2. Profiles used in the study (a) a constant V_s (b) a large-contrast profile (c) a gradually increasing V_s profile

Table 2. Soil profiles used in the current study

Profile #	Depth (m)	V_s (m/s)	V_p (m/s)	ρ (kg/m ³)
Profile 1	0-inf	300	600	1500
Profile 2	0-10	130	260	1400
	10-inf	865	1730	1900
Profile 3	0-3	150	300	1400
	3-6	195	390	1400
	6-9	240	480	1400
	9-12	285	570	1500
	12-15	330	660	1500
	15-18	375	750	1500
	18-21	420	840	1600
	21-24	465	930	1600
	24-27	510	1020	1600
	27-inf	555	1110	1700

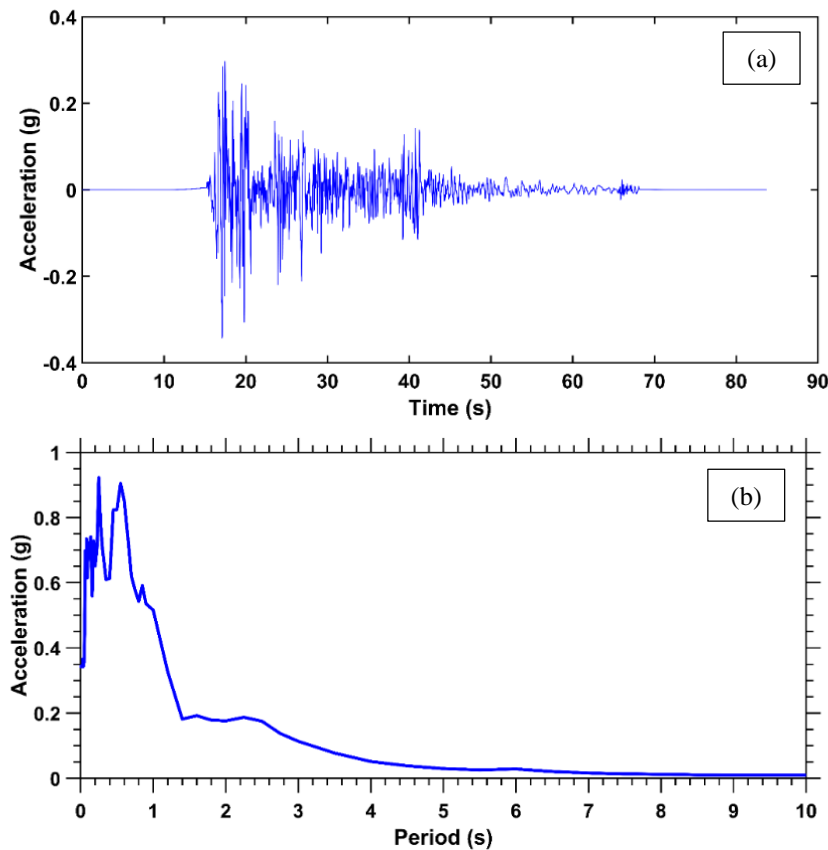


Figure 3. (a) Acceleration time history and (b) response of the 1940 El Centro earthquake

4. Ground Motion Responses and Structural Response

Figures 4 to 6 plot the time histories of acceleration, velocity, and displacements acquired at the ground surface at each site, respectively. As clear on these figures, site effects have led to different responses in each case. According to the acceleration and velocity time histories, profile 3 has had the largest amplification effect on the input motion while profile 1 has shown the least amplifying effect. The magnitude of peak acceleration, peak velocity and peak displacement at each site is summarized in Table 3. A quick comparison according to Table 3 confirms that the peak acceleration at site 3 is about 2.40 times than the observed peak acceleration at site 1. This trend is consistently observed for velocity time histories as well where the site with a gradual increase in stiffness showed a more amplification effect on velocity compared to the other two profiles.

Moreover, the acceleration response from profile 2 (Figure 4) shows that high-frequency components of the input signal (i.e., noise) have been filtered out, and response from this site looks *smoother* than those of the other two sites. This is not surprising; first, as a widely-accepted belief, high-frequency components are substantially more attenuated than components with lower frequencies, and second, soft soils tend to be more attenuative than stiff soils (e.g., [29-31]). Profile 2 is a soft-over-stiff arrangement, and the upper soft part attenuated high frequency components.

Figure 7-a compares the acceleration response spectra at these sites. First, note that profiles 2 and 3 both have increased the expected acceleration response over a wide range of periods compared to the benchmark profile (profile 1). Second, comparing to the benchmark model, profile 3 amplified the expected accelerations but did not change the shape and frequency content of the input motion. On the other hand, profile 2 has changed both the shape and the frequency content of the input motion and has shifted the dominant frequency values to lower frequencies (i.e., longer periods). This observation confirms the speculation that was made earlier that profile 2 tends to filter out the high frequency components and shifts the dominant frequency to a lower range.

Table 3. Ground motion parameters of three profiles

Profile Number	Peak Acceleration (g)	Peak Velocity (m/sec)	Peak Displacement (m)	Predominant Period (sec)
1	0.269	0.287	0.109	0.683
2	0.505	0.485	0.125	0.862
3	0.642	0.556	0.113	0.463

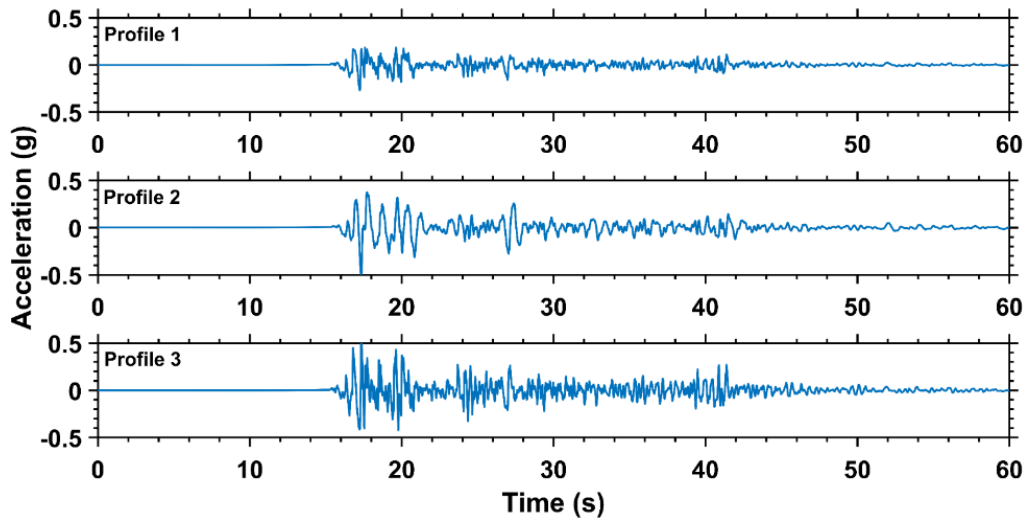


Figure 4. Acceleration time history from the ground motion response

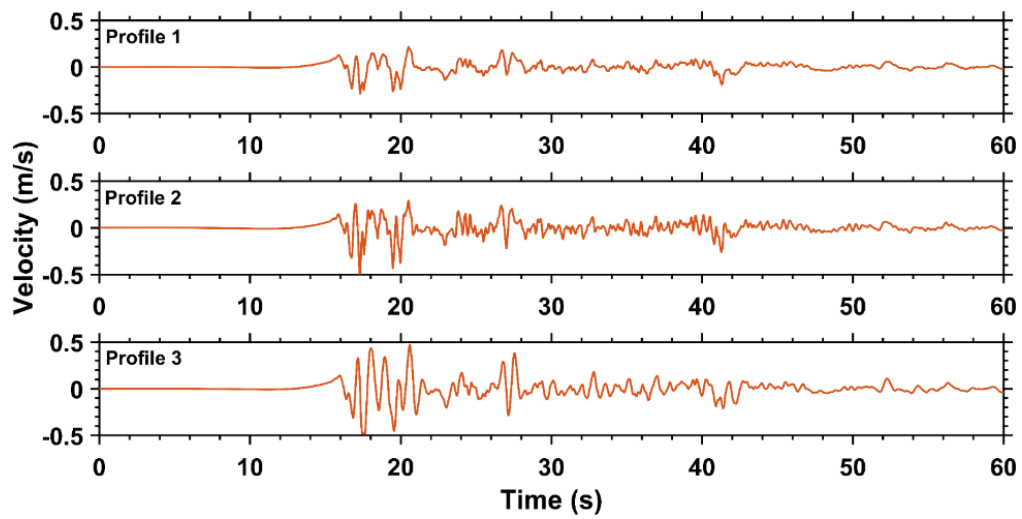


Figure 5. Velocity time history from the ground motion response

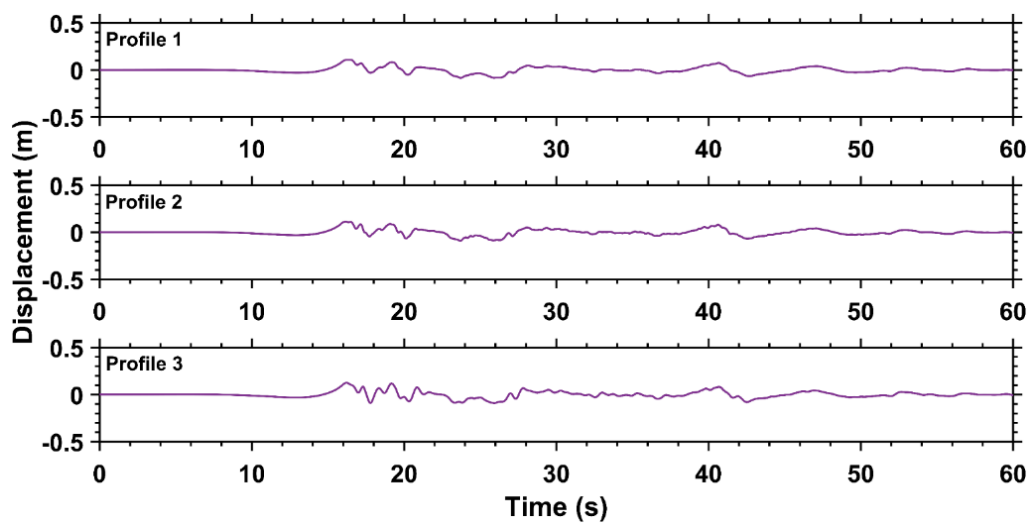


Figure 6. Displacement time history from the ground motion response

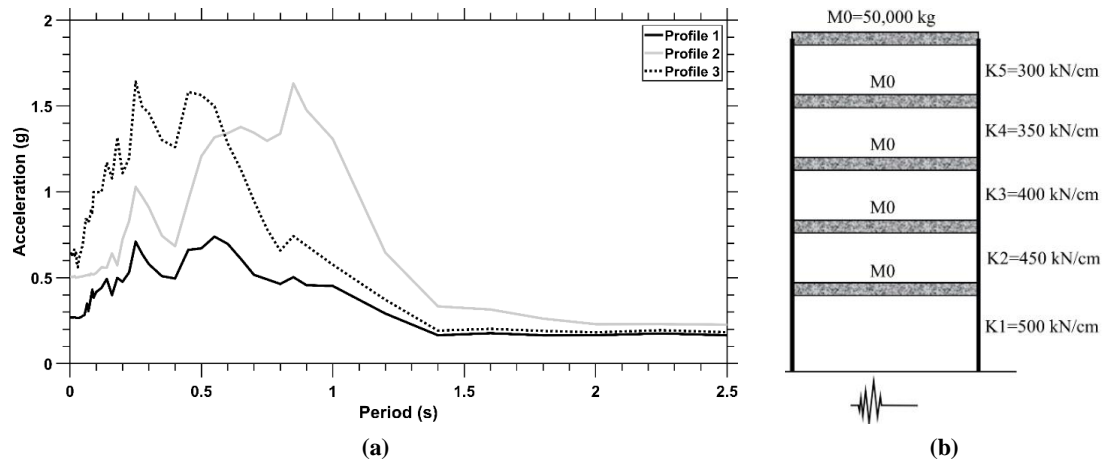


Figure 7. a) Acceleration response spectrum at the ground level; b) 5-DOF structure of the current study

The next step is to investigate how each ground motion response affects an existing structure. In general, the vibration of a multiple-degrees-of-freedom (MDOF) structure subjected to an external (here an earthquake) loading follows the motion presented in Equation 2:

$$M\ddot{u} + C\dot{u} + Ku = -M\ddot{u}_g \quad (2)$$

Where M , C , and K are global mass matrix, damping matrix, and stiffness matrix, respectively, and u is a vector containing the displacements of stories 1 to, n (n being the number of DOFs). \dot{u} and \ddot{u} denote the first and second order derivatives of displacement with respect to time. For a structure with 5 degrees of freedom (Figure 7b), the mass and stiffness matrices are determined using Equations 3 and 4. In Equation 3, m_i denotes the mass of the i^{th} story (here all equal to m_0), and in equation (4), k_i is the stiffness of the i^{th} floor.

$$M = \begin{bmatrix} m_1 & 0 & 0 & 0 & 0 \\ 0 & m_2 & 0 & 0 & 0 \\ 0 & 0 & m_3 & 0 & 0 \\ 0 & 0 & 0 & m_4 & 0 \\ 0 & 0 & 0 & 0 & m_5 \end{bmatrix} \quad (3)$$

$$K = \begin{bmatrix} k_1 + k_2 & -k_2 & 0 & 0 & 0 \\ -k_2 & k_2 + k_3 & -k_3 & 0 & 0 \\ 0 & -k_3 & k_3 + k_4 & -k_4 & 0 \\ 0 & 0 & -k_4 & k_4 + k_5 & -k_5 \\ 0 & 0 & 0 & -k_5 & k_5 \end{bmatrix} \quad (4)$$

The acceleration time histories from Figure 4 were used to excite the 5-story building using the MATLAB script described in the “Methods” section. The contribution of the first 5 modes of displacement were considered in the modal analysis and the displacement time histories of each story for different subsurface scenarios are depicted in Figure 8. The structure is assumed to have a 5% damping ratio. Examining Figure 8 reveals several interesting remarks. First, expectedly, the displacements tend to increase with floor level in all the cases meaning that higher stories experience larger displacements. Second, profiles 2 and 3 (especially 2) have significantly amplified the displacements occurred at stories 3 and above. To illustrate more, note that the displacements at the 5th floor in profile 1 are comparable to those of the 2nd floor in profiles 2 and 3. This shows that identical structures built over soil profiles with the same V_{s30} are likely to experience very different maximum displacements due to the inherent dissimilar subsurface profiles. Finally, although profile 3 yielded the largest PGA at the ground surface level (Table 3), but the structural displacements of profile 2 were significantly larger than those of profiles 1 and 3. A deeper inspection showed that the predominant frequency bandwidth of the input motion at site 2 was more in-line with the natural frequencies of the structure especially with the 1st natural frequency (~ 0.8 Hz) which typically dominates the structural response. Therefore, profile 2 despite having a smaller PGA at the base, imposed a larger displacement on every single story of the structure.

Results of the present study suggest that one can easily underestimate the true peak ground motion parameters that may occur at a site by only relying on the average velocity model, and by not looking at the site-specific conditions such as existence of layers of extremely soft material. Such negligence can lead to devastating damages to the current structures or the structures to be built. Therefore, although V_{s30} provides a promising recommendation for seismic site classification, but experts are strongly encouraged to perform detailed ground motion amplification and response analysis on a case-by-case basis rather than exclusively relying on the V_{s30} value.

5. Conclusion

The average shear-wave velocity of the uppermost 30 meters of earth has found a wide-spread use in the civil engineering field particularly as it relates to seismic site classification, ground motion response, soil-structure interaction, and liquefaction assessments. However, some concerns arise if one only relies on a single parameter to characterize an entire site. Different sites can be considered in the same seismic class due to their similar “average” velocity models, but at the same time, they can exhibit significantly different ground motion responses. In this study, three different soil profiles with an identical V_{s30} were produced. The first profile was a constant-velocity model. The second profile was comprised of a very soft deposit over a stiff layer, and in the third layer, the soil stiffness was gradually increasing with depth. Next, these profiles were subjected to the same ground motion. Then, the corresponding ground motion response were applied to the base of a structure with five degrees of freedom (5 stories). Results indicated that the ground motion response of these sites are different in a meaningful manner. Specifically, the soft-over-stiff profile resulted in the largest structural displacements. This profile also altered the frequency content of the input earthquake the most and shifted the dominant bandwidth to longer periods. It was concluded that practitioners must be cautious when dealing with soft layers as such soils can exhibit unexpected behaviors.

This study reminds us that engineering judgment should always be considered in seismic studies rather than solely relying on V_{s30} to characterize a given site. Otherwise, oversimplification of a site and consolidating all the potential key factors into a single number can lead to underestimating the ground motion amplification that can have detrimental effects on structures. This work can be further extended by performing similar analysis on a much larger pool of velocity models; a Monte Carlo simulation on a large sample space of velocity models with the same V_{s30} can potentially reveal the most critical profiles. A Monte Carlo simulation can also be used in probabilistic risk assessment. However, performing a Monte Carlo simulation of ground motion responses could be a challenging process as it would be time-consuming and computationally-intensive, and requires batch-processing and access to high-performance computing machines.

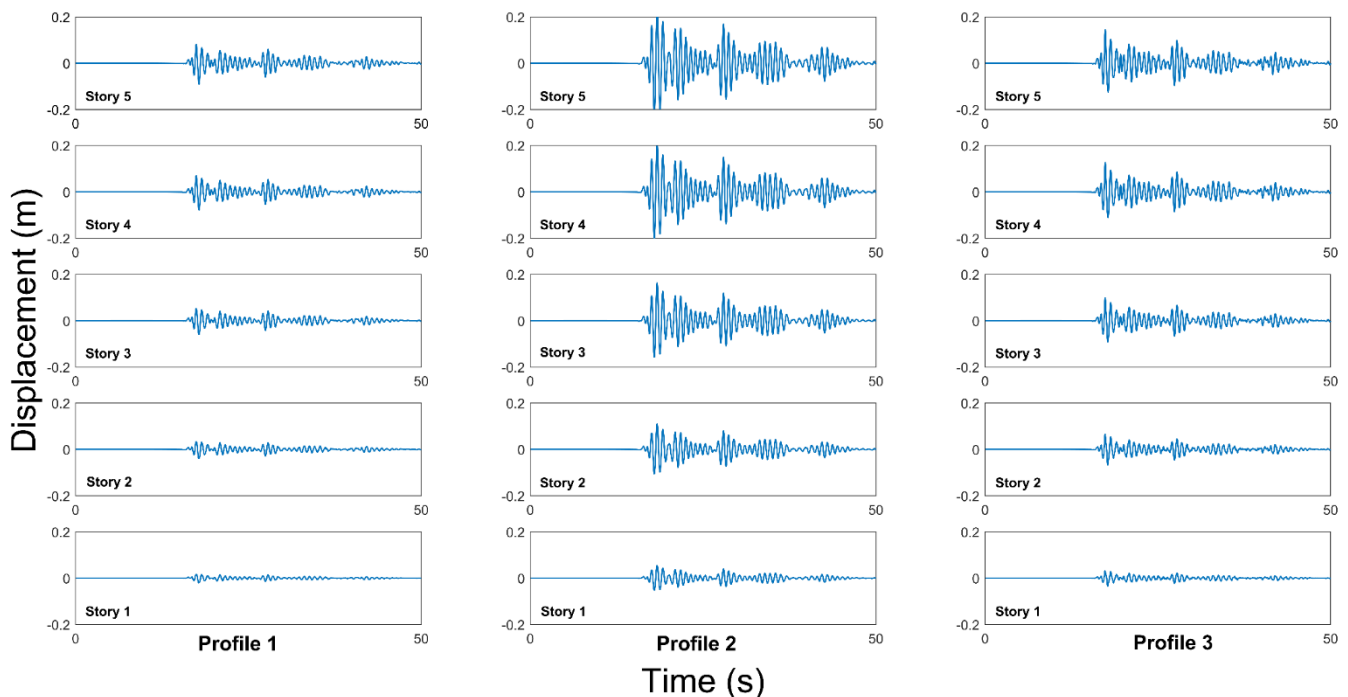


Figure 8. Displacement time histories of the structure over different subsurface profiles

6. Acknowledgements

The authors would like to thank two anonymous reviewers for their valuable comments which helped to improve the quality of the manuscript.

7. Conflicts of Interest

The author declares no conflicts of interest.

8. References

- [1] Foti, Sebastiano, Carlo Lai, Glenn Rix, and Claudio Strobbia. "Surface Wave Methods for Near-Surface Site Characterization" (August 18, 2014). doi:10.1201/b17268.
- [2] Mahvelati, Siavash, Alireza Kordjazi, and Joseph Thomas Coe. "A Review of Seismic Geophysical Testing in Iran for Building Near-Surface Velocity Models." *The Leading Edge* 37, no. 1 (January 2018): 68a1–68a10. doi:10.1190/tle37010068a1.1.
- [3] Butler, Dwain K., ed. "Near-Surface Geophysics" (January 2005). doi:10.1190/1.9781560801719.
- [4] Imai, T., and Tonouchi, K. "Correlation of N value with S-wave velocity and shear modulus." *Proceedings of the 2nd European Symposium on Penetration Testing*, Amsterdam, 24-27 May.
- [5] Sykora, D. W., and K. H. I. I. Stokoe. "Correlations of in situ measurements in sands of shear wave velocity, soil characteristics, and site conditions, Report GR 83-33." Civil Engineering Department, University of Texas at Austin (1983).
- [6] Pitilakis, K., D. Raptakis, K. Lontzetidis, Th. Tika-Vassilikou, and D. Jongmans. "Geotechnical and Geophysical Description of Euro-Seistest, Using Field, Laboratory Tests and Moderate Strong Motion Recordings." *Journal of Earthquake Engineering* 3, no. 3 (July 1999): 381–409. doi:10.1080/13632469909350352.
- [7] Brandenberg, Scott J., Naresh Bellana, and Thomas Shantz. "Shear Wave Velocity as Function of Standard Penetration Test Resistance and Vertical Effective Stress at California Bridge Sites." *Soil Dynamics and Earthquake Engineering* 30, no. 10 (October 2010): 1026–1035. doi:10.1016/j.soildyn.2010.04.014.
- [8] Hunter, J. A., S. E. Pullan, R. A. Burns, R. L. Good, J. B. Harris, A. Pugin, A. Skvortsov, and N. N. Goriainov. "Downhole Seismic Logging for High - resolution Reflection Surveying in Unconsolidated Overburden." *GEOPHYSICS* 63, no. 4 (July 1998): 1371 – 1384. doi:10.1190/1.1444439.
- [9] Xia, Jianghai, Richard D. Miller, Choon B. Park, James A. Hunter, and James B. Harris. "Comparing Shear-Wave Velocity Profiles from MASW with Borehole Measurements in Unconsolidated Sediments, Fraser River Delta, B.C., Canada." *Journal of Environmental and Engineering Geophysics* 5, no. 3 (September 2000): 1–13. doi:10.4133/jee5.3.1.
- [10] Penumadu, Dayakar, and Choon B. Park. "Multichannel Analysis of Surface Wave (MASW) Method for Geotechnical Site Characterization." *Earthquake Engineering and Soil Dynamics* (October 9, 2005). doi:10.1061/40779(158)3.
- [11] Socco, Laura Valentina, Sebastiano Foti, and Daniele Boiero. "Surface-Wave Analysis for Building Near-Surface Velocity Models — Established Approaches and New Perspectives." *Geophysics* 75, no. 5 (September 2010): 75A83–75A102. doi:10.1190/1.3479491.
- [12] Mahvelati, Siavash, and Joseph Thomas Coe. "Multichannel Analysis of Surface Waves (MASW) Using Both Rayleigh and Love Waves to Characterize Site Conditions." *Geotechnical Frontiers 2017* (March 30, 2017). doi:10.1061/9780784480441.068.
- [13] Inazaki, T. "High-Resolution S-Wave Reflection Survey in Urban Areas Using a Woven Belt Type Land Streamer." *Near Surface 2006 - 12th EAGE European Meeting of Environmental and Engineering Geophysics* (September 4, 2006). doi:10.3997/2214-4609.201402656.
- [14] Olona - Allué, Javier, Javier A. Pulgar, Gabriela Fernández - Viejo, and Juan M. González - Cortina. "Geotechnical Site Characterization of a Flood Plain by Refraction Microtremor and Seismic Refraction Methods." *Symposium on the Application of Geophysics to Engineering and Environmental Problems 2008* (January 2008). doi:10.4133/1.2963283.
- [15] Maheswari, R. Uma, A. Boominathan, and G.R. Dodagoudar. "Seismic Site Classification and Site Period Mapping of Chennai City Using Geophysical and Geotechnical Data." *Journal of Applied Geophysics* 72, no. 3 (November 2010): 152–168. doi:10.1016/j.jappgeo.2010.08.002.
- [16] Louie, J. N., S. K. Pullammanappallil, A. Pancha, T. West, and W. K. Hellmer. "Earthquake Hazard Class Mapping by Parcel in Las Vegas Valley." *Structures Congress 2011* (April 13, 2011). doi:10.1061/41171(401)156.
- [17] Coe, Joseph, Michael Senior, Siavash Mahvelati, and Philip Asabere. "Preliminary Development of a Seismic Microzonation Map of Philadelphia Using Surface Wave Testing and Data from Existing Geotechnical Investigations." *Symposium on the Application of Geophysics to Engineering and Environmental Problems 2015* (March 24, 2016). doi:10.4133/sageep.29-030.
- [18] FEMA. "NEHRP recommended provisions (National Earthquake Hazards Reduction Program) for seismic regulations for new buildings and other structures (FEMA 450)" (2003).
- [19] Wald, D.J., McWhirter, L., Thompson, E., and Hering, A.S. "A new strategy for developing Vs30 maps" *Proceedings of the 4th IASPEI/IAEE International Symposium: Effects of Surface Geology on Seismic Motion*, Santa Barbara, CA.
- [20] Godfrey, Elizabeth A., Adrian Rodriguez-Marek, and C. Guney Olgun. "Probabilistic Methodology for Developing Regional and Site-Class Dependent Seismic Site Amplification Factors." *IFCEE 2015* (March 17, 2015). doi:10.1061/9780784479087.173.
- [21] Aboye, Shimelies A., Ronald D. Andrus, Nadarajah Ravichandran, Ariful H. Bhuiyan, and Nicholas Harman. "Seismic Site Factors and Design Response Spectra Based on Conditions in Charleston, South Carolina." *Earthquake Spectra* 31, no. 2 (May 2015): 723–744. doi:10.1193/041912eqs163m.
- [22] Hartzell, S. "Site Response, Shallow Shear-Wave Velocity, and Damage in Los Gatos, California, from the 1989 Loma Prieta Earthquake." *Bulletin of the Seismological Society of America* 91, no. 3 (June 1, 2001): 468–478. doi:10.1785/0120000235.

- [23] Frankel, A. D. "Nonlinear and Linear Site Response and Basin Effects in Seattle for the M 6.8 Nisqually, Washington, Earthquake." *Bulletin of the Seismological Society of America* 92, no. 6 (August 1, 2002): 2090–2109. doi:10.1785/0120010254.
- [24] Hartzell, S. "Site Response, Shallow Shear-Wave Velocity, and Wave Propagation at the San Jose, California, Dense Seismic Array." *Bulletin of the Seismological Society of America* 93, no. 1 (February 1, 2003): 443–464. doi:10.1785/0120020080.
- [25] Castellaro, S., F. Mulargia, and P. L. Rossi. "Vs30: Proxy for Seismic Amplification?" *Seismological Research Letters* 79, no. 4 (July 1, 2008): 540–543. doi:10.1785/gssrl.79.4.540.
- [26] Seed, H.B., and Idriss, I.M. "Soil moduli and damping factors for dynamic response analyses. Report No. EERC 70-10" (1970) Earthquake Engineering Research Center, Berkeley.
- [27] Tazarv, M. "Modal Time History Analysis of Structures" Retrieved from https://www.mathworks.com/matlabcentral/fileexchange/30866-modal-time-history-analysis-of-structures?s_tid=prof_contriblnk.
- [28] Ludwig, W.J., Nafe, J.E., and Drake, C.L. "Seismic refraction." *The Sea* (1970) A. E. Maxwell, (Editor), Wiley-Interscience, New York.
- [29] Hu, Jia-Fu, and You-Jin Su. "Estimation of the Quality Factor in Shallow Soil Using Surface Waves." *Acta Seismologica Sinica* 12, no. 4 (July 1999): 481–487. doi:10.1007/s11589-999-0089-z.
- [30] Badsar, S. A., M. Schevenels, W. Haegeman, and G. Degrande. "Determination of the Material Damping Ratio in the Soil from SASW Tests Using the Half-Power Bandwidth Method." *Geophysical Journal International* 182, no. 3 (July 8, 2010): 1493–1508. doi:10.1111/j.1365-246x.2010.04690.x.
- [31] Igel, H. "Computational seismology a practical introduction" (2018). Oxford University Press.